JOURNAL OF SOLID STATE CHEMISTRY **123,** 203–207 (1996)
ARTICLE NO. 0169

The Ternary System Au–Ni–Sn

Alexandra Neumann, A. Kjekshus,[1] and E. Røst

Department of Chemistry, University of Oslo, Blindern, N-0315 Oslo, Norway

Received September 1, 1995; accepted January 23, 1996

The phase relations in the Au–Ni–Sn system have been examined by powder X-ray diffraction, metallography, electron microprobe analysis, and thermal analysis. The range of homogeneity of the various phases, tie-lines, and tie-triangles are presented for an isothermal section of the phase diagram at 400°C. Au and Ni can scarcely be mutually exchanged in most of the phases, but a continuous range of solid solubility seemingly occurs between AuSn (δ) and Ni_3Sn_2 (γ). The maximum variation in the Sn content for this phase is found to be ca. 5 at%, for mole fractions between $n_{Ni}/(n_{Au} + n_{Ni}) = 0.7$ and 1.0. The only genuine ternary phase in the system, labeled A, takes the virtually stoichiometric composition $AuNi_2Sn_4$ and exists at 400°C.

INTRODUCTION

This report concerns the mapping of the ternary system Au–Ni–Sn and represents a continuation of our account of the crystal structure $AuNi_2Sn_4$ (1). Like other tin systems, Au–Ni–Sn has provided a number of challenging characterization problems—for metallography and X-ray diffraction in particular.

As a background, it is convenient to recall the binary phase diagrams of Au–Ni, Au–Sn, and Ni–Sn. Au and Ni form a continuous solubility above 810°C. At 400°C there is a miscibility gap from ca. 7 to 99 at% Ni according to Okamoto and Massalski (2). The Au–Sn system is described by Karlsen *et al.* (3). The phase diagram for Ni–Sn compiled by Nash and Nash (4), contains three binary phases at 400°C: Ni_3Sn (β), Ni_3Sn_2 (γ) and Ni_3Sn_4 (δ), all with fairly narrow homogeneity ranges. Further information on these phases will be provided in the results section. Reference (4) indicates a solid solubility of ca. 2 at% Sn in Ni (α) and a corresponding solubility of Ni in liquid (L) Sn at 400°C.

[1] To whom correspondence should be addressed.

EXPERIMENTAL

Samples were made by melting (heating at 1100–1300°C for ca. 1 min under vigorous shaking) weighed amounts of 99.95% Au (Rasmussen), 99.98% Ni (Goodfellow), and 99.98% Sn (Merck) in sealed, evacuated, silica-glass tubes. This initial heat treatment was in most cases concluded by quenching the samples from the molten state into water, otherwise cooled slowly to room temperature. Most samples were then annealed at 400°C (for 2–7 days) and then quenched into water. The Ni-rich samples were annealed for a minimum of 7 days because of the high melting temperatures in this region of the phase diagram.

Specimens for X-ray powder diffraction (PXD) were obtained by crushing one part of the sample to a fine powder. For ductile samples filing and subsequent annealing at 250–400°C for 6–8 hr was necessary to obtain powder suitable for PXD. All samples were checked for homogeneity and characterized by PXD using Guinier–Hägg cameras with Cu$K\alpha_1$ radiation and Si as internal standard. Position and intensity measurements were carried out using a Nicolet L18 film scanner controlled by the SCANPI program system (6). Unit-cell parameters were obtained using the CELLKANT program (7).

Differential thermal analysis (DTA) measurements were carried out using Perkin–Elmer 7 Series Thermal Analysis System. Samples (50–150 mg) contained in sealed glass tubes were heated at a rate of 5°C min^{-1} between 20 and 1000°C.

Metallographic cross sections were obtained by mounting 2–3 pieces of specimen, taken from different parts of the sample, in resin (Struers No. 3). Grinding was carried out using silicon carbide paper under water cooling, and polishing according to Struers DP procedure. Cross sections used for optical microscopy were usually etched with either a mixture of $FeCl_3$ and HCl in water or 6*M* HCl. A thin layer of carbon was evaporated on the specimens used for electron microscopy. Optical microscopy was performed on a PME Olympus microscope, and electron microprobe (MP) analysis on a wave-

0022-4596/96 $18.00

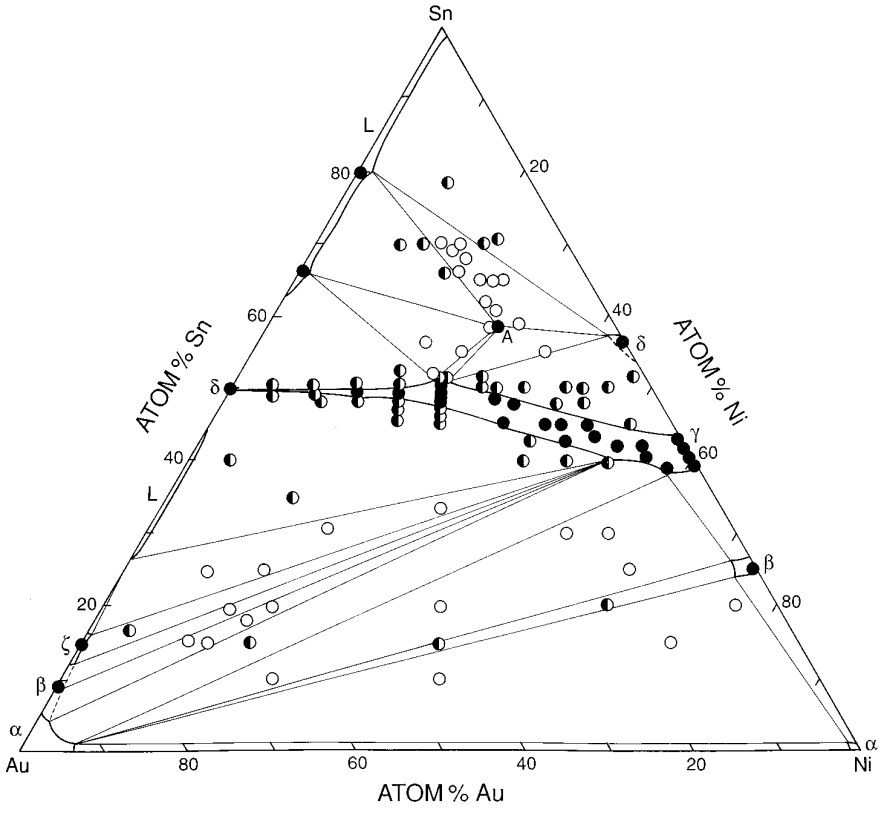

FIG. 1. Locations of selected (relevant) samples in the Au–Ni–Sn triangle. Filled, half-filled, and open circles represent samples containing one, two, and three phases, respectively, after annealing at 400°C. Phase limits, tie-lines, and tie-triangles determined by direct experiments are marked by solid lines.

length dispersive Cameca Electron Microprobe with a LINK energy dispersive system. Matrix corrections were carried out using a PAP procedure which is included in the Cameca software.

ISOTHERMAL SECTION AT 400°C

A major part of this report concerns the isothermal section at 400°C. Figure 1 gives the location of the most relevant samples used for the determination of the phase relations in the Au–Ni–Sn system. Different symbols are used to mark whether these are established as one, two, or three phase at 400°C. The experimentally determined (by metallography, microprobe analysis, and/or comparisons of unit-cell dimensions) ranges of homogeneity, together with tie-lines and tie-triangles at 400°C are shown in Fig. 2. The designations for the binary phases follow Refs. (2–4, 8) and the phase which extends from AuSn (δ) to Ni_3Sn_2 (γ) is referred to as δ/γ. Since there could arise some confusion concerning the β phases (in both the Au–Sn and Ni–Sn system), these will be denoted Au-based β and Ni-based β. The genuine ternary phase is designated A.

The α phases. Au dissolves ca. 7 at% Ni and ca. 6 at% Sn; Ni ca. 1 at% of each of Au and Sn at 400°C. Both phases take the same Cu-type fcc structure. The solid-solubility ranges of the α phases increase with increasing temperature.

The Au-based β and ζ phases. There is very little solid solubility of Ni in both these phases, according to MP analysis below 1 at% Ni. The solid solubility with respect to Sn is of the same magnitude as in the binary system.

The Ni-based β phase. The Ni-based β phase takes the Mg_3Cd-type structure and dissolves about 4.4 at% Au. This gives rise to a minute increase in the unit-cell dimensions, but the changes are considered too small to deserve extensive measurements.

The δ/γ phase. The δ/γ phase has an extended homogeneity range from AuSn (δ) to Ni_3Sn_2 (γ) at 400°C, and its crystal structure ranges from NiAs-type to partly filled NiAs–Ni_2In-type. On the Ni-rich side there is a subfield with a superstructure (marked in Fig. 2; originating from γ' in the binary Ni–Sn system). The boundary between the subfield and the main δ/γ phase field is probably of second order, but this and other details concerning the superstructure are left for a separate study. The homogene-

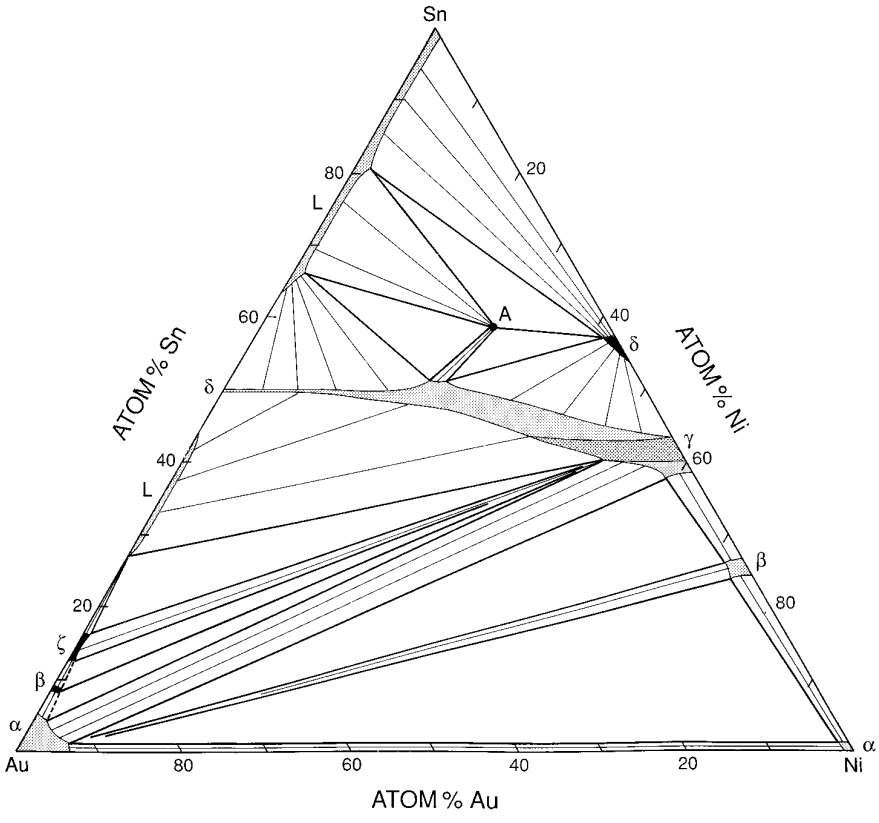

FIG. 2. Isothermal cross section of the Au–Ni–Sn phase diagram at (or near) 400°C. One-phase regions appear as shaded or black areas, thick lines or points, two-phase regions are shown by tie-lines, and three-phase fields are exhibited by open tie-triangles. The superstructure of δ/γ appears as a darker shade in the δ/γ-phase field.

ity range widens appreciably with respect to the Sn content on going from AuSn to Ni_3Sn_2. At, say, the equiatomic Ni/Au ratio the homogeneity range extends from ca. 47 to 50 at% Sn at 400°C. Figure 3 shows the variation in the unit-cell dimensions of the δ/γ phase, both as a function of the mole fraction $n_{Ni}/(n_{Au} + n_{Ni})$ and with respect to the Sn content for $n_{Ni}/(n_{Au} + n_{Ni}) = 0.5$. The dashed-dotted lines on the Ni-rich side of Fig. 3 correspond to the superstructure field and here the experimental points refer to samples which have been annealed at higher temperature where the structure is hexagonal. The broken-line sections represent a composition range where it has proved difficult to obtain homogeneous samples by annealing at 400°C. The general impression is that the unit-cell dimensions decrease both with increasing $n_{Ni}/(n_{Au} + n_{Ni})$ and increasing Sn content. However, on the Sn-rich side of the limiting lattice-parameter relationships in the inset to Fig. 3 there occur approximately horizontal sections which reflect the variation in shape of the phase boundary in Fig. 2.

The results summarized in Fig. 2 show that there is very slight variation in the Sn content on the Au-rich side of the δ/γ phase, and more extensive variation on the Ni-rich side where Ni_3Sn_2 itself extends from 38.5 to 42.5 at% Sn. These findings fully comply with Refs. (9, 10).

The Ni-based δ phase. The present report is based on the results of Furuseth and Fjellvåg (11) and Bhargava and Schubert (12) who both maintain that the δ phase extends from 52.6 to 56.5 at% Sn at 273 K. References (11, 12) moreover introduce an additional NiSn (δ') phase in the range 51.4 and 52.0 at% Sn at 273 K. This latter phase is not found in our ternary samples at 400°C. Whether this reflects our annealing temperature or a complete lack of solid solubility of Au in NiSn is not clarified, but NiSn is not included in Fig. 2.

The crystal structure of the δ phase represents really a separate prototype, but it is often classified among the Cr_3S_4-type structure. (For the NiSn phase, Furuseth and Fjellvåg (11) report a monoclinic unit cell, whereas Bhargava and Schubert (12) maintain that the unit cell is orthorhombic.)

The homogeneity range of the δ phase at 400°C is stipulated to be between 52.6 at% Sn at the lower Sn limit where virtually no Au is dissolved and 57.7 at% Sn at the higher Sn limit where approximately 1 at% Au dissolves. The high

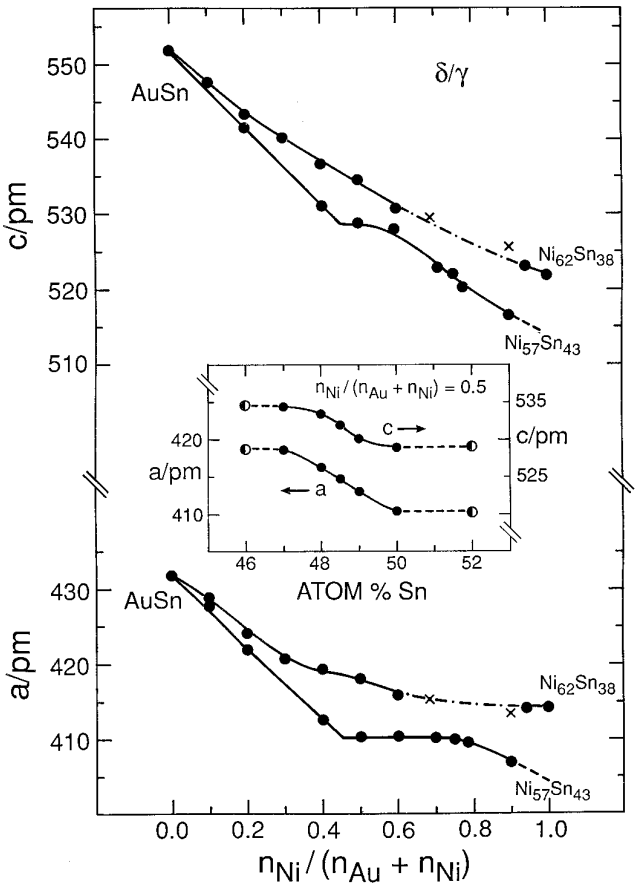

FIG. 3. Unit-cell dimensions as a function of $n_{Ni}/(n_{Au} + n_{Ni})$ mole fraction for the δ/γ phase (Ni-poor and Ni-rich limits; samples annealed at 400°C). Estimated error limits do not exceed the size of the symbols. Points marked ● represent one-phase samples, points marked × belong to the superstructure region at 400°C and these data refer to a higher annealing temperature (600°C, where the hexagonal NiAs–Ni_2In-type arrangement is stable). Dashed-dotted lines indicate the region with the superstructure. The inset shows unit-cell dimensions as a function of at% Sn for samples with mole fraction $n_{Ni}/(n_{Au} + n_{Ni}) = 0.5$. Half-filled circles represent two-phase samples, and broken lines two-phase region.

melting temperatures for δ (melts peritectically at 795°C) and δ/γ (melts congruently at 1264°C) cause problems in the equilibration of the samples.

The melt phases. Two separate melt phases occur in the Au–Ni–Sn phase diagram at 400°C (Fig. 2). None of these melts dissolve appreciable amounts of Ni (ca. 1 at% Ni at most). One of the melts extends at 400°C from 26 to 45 at% Sn, and the other from 57 to 100 at% Sn. The extention of the melt regions were determined by metallography and MP analyses. When a sample which is partly molten at 400°C is quenched, the melt solidifies as a fine grained matrix which is easily detectable by optical and electron microscopy. The composition of the matrix represents the composition of the melt, which in turn is determined by MP analysis.

The A phase. Identificational documentation and structural data for the A phase are given in Ref. (1). The A phase is virtually stoichiometric with the composition $AuNi_2Sn_4$ and the crystal structure of this phase is of the Fe_3S_4–*s*-type (1, 5) with $a = 422.6(1)$ and $c = 2656.6(4)$ pm in hexagonal setting.

DEVELOPMENT OF SOLIDUS AND LIQUIDUS FOR δ/γ

The congruent melting point of δ and γ is 419.3 and 1264°C, respectively. Several samples of the δ/γ phase have been subject to thermal analysis in order to map solidus and liquidus temperatures, but with meager results. The cause of the problem is partly on the instrumental side and partly owing to the extended melting interval of the δ/γ phase.

Data for the solidus and liquidus boundaries are there-

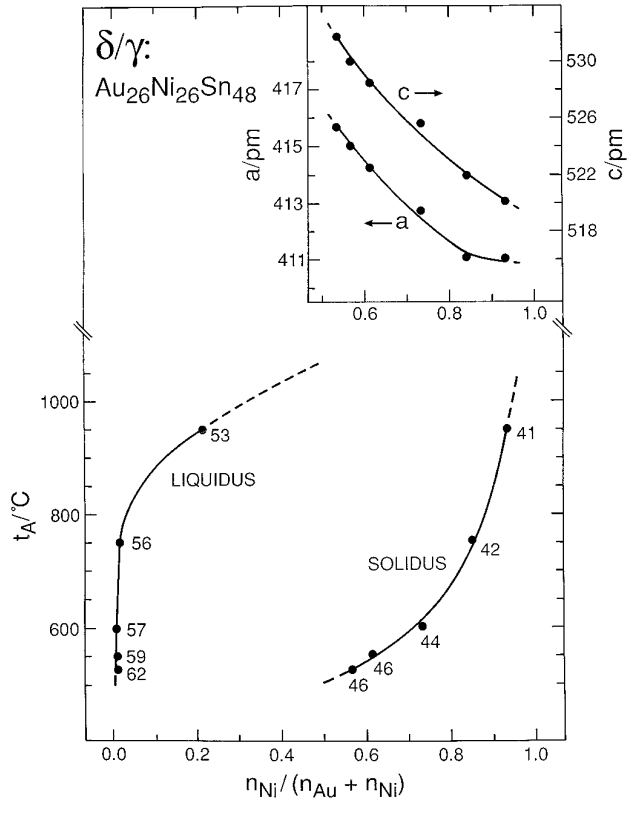

FIG. 4. Liquidus and solidus curves as a function of $n_{Ni}/(n_{Au} + n_{Ni})$ mole fraction for samples from the δ/γ-phase field, all with nominal composition $Au_{26}Ni_{26}Sn_{48}$. t_A represents the annealing temperatures. The numbers attached to the points on liquidus and solidus give the Sn content in at% as determined by MP. Estimated error limits do not exceed the size of the symbols on the liquidus and solidus curves. The inset shows unit-cell dimensions as a function of $n_{Ni}/(n_{Au} + n_{Ni})$. (The nominal $Au_{26}Ni_{26}Sn_{48}$ samples were annealed at different temperatures and quenched to room temperature.) Here the error limits may exceed the size of the symbols.

fore limited to samples with the nominal composition $Au_{26}Ni_{26}Sn_{48}$. The mapping is based solely on annealing and quenching experiments from different temperatures; measurements being performed by MP analysis on primary precipitated crystals of δ/γ and melt. The melting in this region starts at 515°C and the last crystals dissolve between 1000 and 1050°C. The melt contains around 1 at% Ni up to 750°C, which is manifested in the very steep liquidus curve in Fig. 4. This is in complete agreement with the observed lack of solubility of Ni in the melt phases at 400°C. The tie-line directions in the two-phase region δ/γ–melt may change with the composition, and, hence, only the tie-lines through the nominal $Au_{26}Ni_{26}Sn_{48}$ sample are determined experimentally. As seen from Fig. 4 the Sn content (specified on the illustration) decreases with the temperature for both liquidus and solidus.

CONCLUDING CONSIDERATIONS

A characteristic feature of the Au–Ni–Sn system is the lack of solid solubility in the Au–Ni dimension. This is not surprising, since well established criteria for the occurrence of solid solubility are not satisfied. The size difference between Au and Ni is well outside the 15% criterion of Hume–Rothery (13). This also shows up in the Au–Ni phase diagram where there is a large miscibility gap at 400°C, and complete solid solubility is only obtained in a ca. 150°C interval above ca. 810°C. The metallic valences of Au and Ni are very different, and the difference in electronegativity does not promote the solid solubility either. The lack of solid solubility is also reflected in the virtually stoichiometric phase A. Even the two (Au anchored) melt regions in the Au–Ni–Sn diagram at 400°C show very little solubility of Ni, and the melts are in fact extremely Ni-poor up to about 750°C. In apparent contradiction to this, the δ/γ phase forms a continuous solid-solution range at 400°C. However, this feature concurs with the well established fact that the NiAs–Ni_2In-type structure can tolerate extensive variations in composition (14).

ACKNOWLEDEGMENT

The authors are grateful to Dr. H. Austrheim (Mineralogical Geological Museum, University of Oslo) for assistance with electron microprobe analyses.

REFERENCES

1. A. Neumann, A. Kjekshus, C. Rømming, and E. Røst, *J. Solid State Chem.* **119,** 142 (1995).
2. H. Okamoto and T. B. Massalski, ''Binary Alloy Phase Diagrams,'' American Society for Metals, Metals Park, OH, 1990.
3. O. B. Karlsen, A. Kjekshus, and E. Røst, *Acta Chem. Scand.* **46,** 147 (1992).
4. P. Nash and A. Nash, ''Binary Alloy Phase Diagrams,'' American Society for Metals, Metals Park, OH, 1990.
5. C. R. Erd, M. T. Evans, and D. H. Richter, *Am. Mineral.* **42,** 309 (1958).
6. P.-E. Werner, ''The Computer Program SCANPI,'' Institute of Inorganic Chemistry, University of Stockholm, Sweden, 1981.
7. N. O. Ersson, ''Program CELLKANT,'' Chemical Institute, Uppsala University, Uppsala, Sweden, 1981.
8. F. Lihl and H. Kirnbauer, *Monatsh. Chem.* **86,** 745 (1955).
9. J.-P. Jan, W. B. Pearson, A. Kjekshus, and S. B. Woods, *Can. J. Phys.* **41,** 2252 (1963).
10. H. Fjellvåg and A. Kjekshus, *Acta Chem. Scand. A* **40,** 23 (1986).
11. S. Furuseth and H. Fjellvåg, *Acta Chem. Scand. A* **40,** 695 (1986).
12. M. K. Bhargava and K. Schubert, *J. Less-Common Met.* **33,** 181 (1973).
13. W. B. Pearson, ''The Crystal Chemistry and Physics of Metals and Alloys,'' Wiley–Interscience, New York, 1972.
14. A. Kjekshus and W. B. Pearson, *Progr. Solid State Chem.* **1,** 83 (1964).